Chaos and Bifurcations in Periodic Windows Observed in Plasmas

J. Qin, L. Wang, D. P. Yuan, P. Gao, and B. Z. Zhang
Institute of Physics, Academia Sinica, Beijing, China
(Received 12 December 1988)

We report the experimental observations of deterministic chaos in a steady-state plasma which is not driven by any extra periodic forces. Two routes to chaos have been found, period-doubling and intermittent chaos. The fine structures in chaos such as periodic windows and bifurcations in windows have also been observed.

PACS numbers: 52.35.Ra, 05.45.+b, 52.80.−s

Since deterministic chaos was discovered by Lorenz[1] in numerical simulations, the subject has attracted much attention in many fields.[2,3] In the case of physics, many experimental studies on chaos have been performed in nonautonomous systems such as nonlinear circuits,[4] or in time-delayed systems such as nonlinear optics.[5] The chaotic behavior of the systems was determined by the frequency and intensity of period-driven forces or by the feedback term of time delay. Such chaotic behavior may thus be classed as "driven chaos." Recently, driven chaos in plasma has also been observed.[6,7] In this Letter we report experimental observations of deterministic chaos occurring in an undriven plasma system. Two routes to chaos have been found, period-doubling and intermittent chaos. Fine structures such as periodic windows embedded in chaos and bifurcations occurring in the periodic windows have also been observed. The plasma oscillation is a kind of self-generated oscillation because the plasma system is not driven by any extra periodic forces. The fundamental frequency of self-oscillations varies with the changes of control parameters in the discharge, and there is no defined frequency that can be referred to in the system. So here, plasma chaos may be classed as "undriven chaos." The Lorenz chaos is a theoretical example of undriven chaos.

The experimental apparatus is schematically shown in Fig. 1. A cylindrical stainless-steel chamber 80 cm in diameter and 160 cm in length is surrounded by rows of permanent magnets on its surface to form a steady-state plasma device. The chamber is evacuated to a base pressure of 1.5×10^{-6} Torr and filled with argon as a working gas. Tens of tungsten filaments are connected in parallel to two copper rings 40 cm in diameter which are located at one end of the chamber. The primary electrons emitted from hot filaments are accelerated to ionize the background-neutral argon gas to produce a plasma. The discharge is controlled by the argon pressure (P_a), the filament current (I_f), and the discharge voltage (V_d) which biases the filaments negatively with respect to the grounded chamber wall. The main diagnostic apparatus involves movable single Langmuir probes. Typical plasma parameters in this device are

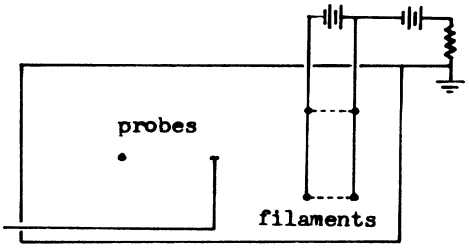

FIG. 1. Schematic of experimental apparatus.

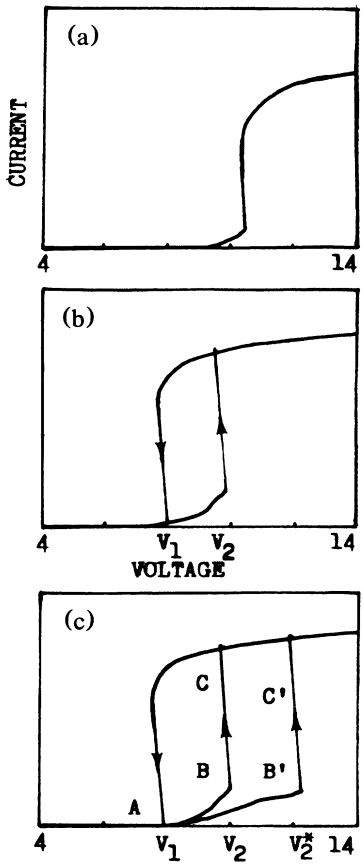

FIG. 2. Current-voltage characteristic of discharge obtained at $I_f=240$ A and (a) $P_a<1\times10^{-4}$ Torr; (b) $P_a=8\times10^{-4}$ Torr; (c) $P_a=1.5\times10^{-3}$ Torr.

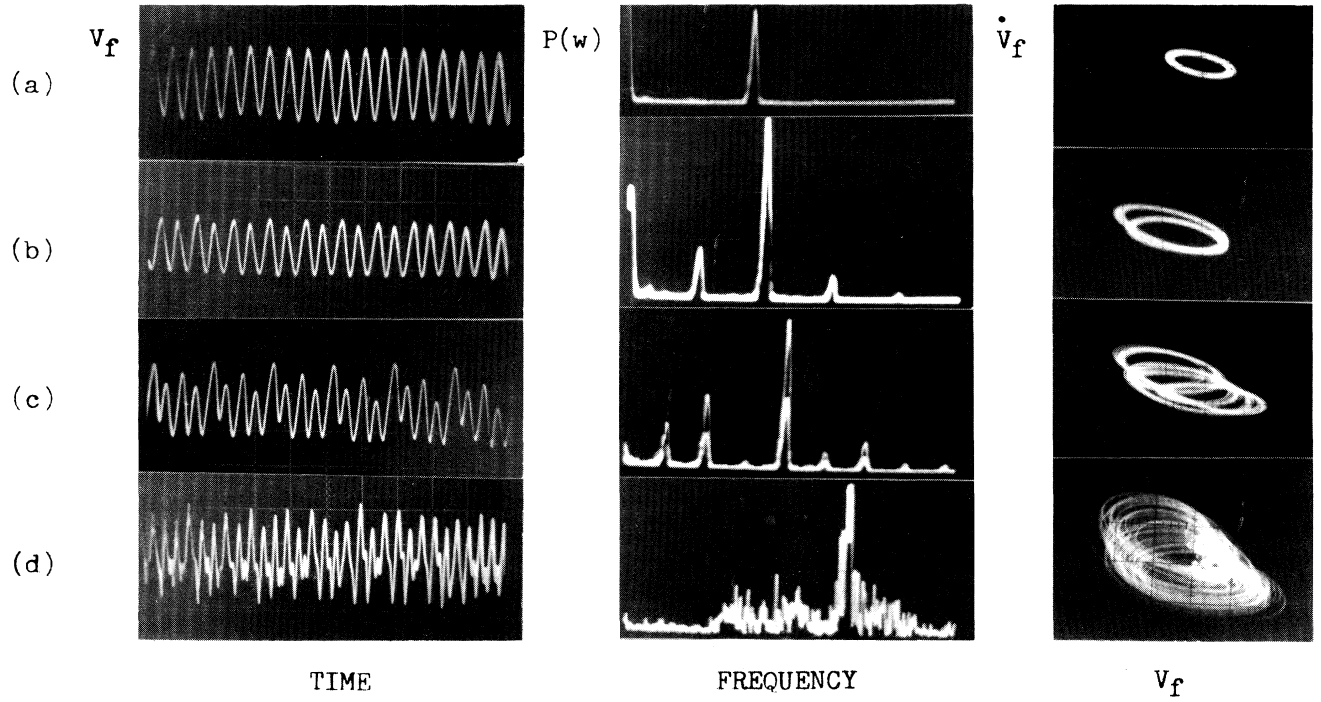

FIG. 3. A period-doubling sequence to chaos observed at $I_f = 240$ A, $P_a = 2.4 \times 10^{-3}$ Torr. The temporal evolution of the potential of unbiased probes, the power spectra, and the trajectory in phase space $(V_f, \dot{V}_f)$ is shown. (a) $V_d = 7.35$ V; (b) $V_d = 7.55$ V; (c) $V_d = 7.80$ V; (d) $V_d = 8.44$ V.

$T_e = 2$-3 eV and $N_e = 10^7$-10^9 cm^{-3}, where T_e and N_e are the plasma electron temperature and density, respectively.

The experiments are performed in the following way. For given values of P_a and I_f, the current-voltage characteristics of the discharge can be plotted on an X-Y recorder by changing the discharge voltage. Figure 2 shows typical results obtained at $I_f = 240$ A and different values of argon pressure. At small values of pressure, the discharge current (I_d) varies monotonically with the discharge voltage [Fig. 2(a)]. When the pressure is increased above 1×10^{-4} Torr, hysteresis occurs in the current-voltage curve, and the higher the pressure is, the more obvious hysteresis becomes [Fig. 2(b)]. When the pressure is further increased above 9×10^{-4} Torr, the hysteresis curve begins to have two lower branches labeled by $A \rightarrow B \rightarrow C$ and $A \rightarrow B' \rightarrow C'$ through bifurcation [Fig. 2(c)]. This bifurcation is stochastic in the pressure range of $(0.9$-$2.5) \times 10^{-3}$ Torr. This means that of the two lower branches the one the current will follow is purely stochastic in the above pressure range, but at a lower pressure the probability for the $A \rightarrow B \rightarrow C$ branch to appear is larger than that for the $A \rightarrow B' \rightarrow C'$ branch, whereas at a higher pressure the situation is just reversed. When the pressure is increased above 2.5×10^{-3} Torr, the $A \rightarrow B \rightarrow C$ branch will disappear.

Following the branch $A \rightarrow B' \rightarrow C'$ before the current jump in the I-V curve, the discharge may display chaotic behavior through period doubling or intermittency. At first, the discharge state is stationary. The signals of discharge current I_d, the floating potential of an un-

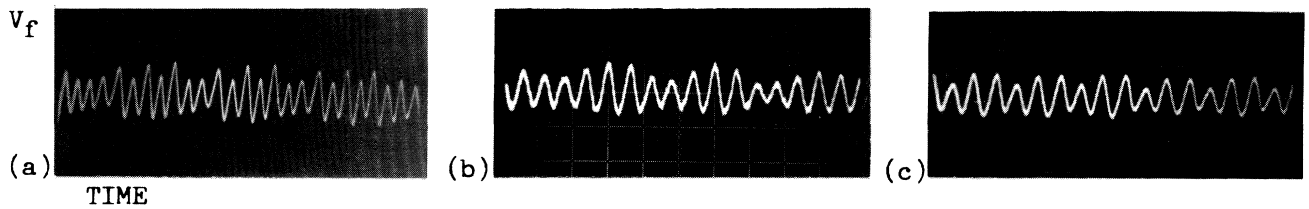

FIG. 4. Some periodic windows observed at $I_f = 240$ A, $P_a = (1$-$1.7) \times 10^{-3}$ Torr. (a) $7P$: $V_d = 9.39$ V; (b) $5P$: $V_d = 9.60$ V; (c) $3P$: $V_d = 9.96$ V.

biased probe V_f, and I_{es}, the electron saturation current of the probe biased positively above the plasma potential, are all dc values. As V_d is increased above a certain threshold value, I_d, V_f, and I_{es} all become "self-generated" oscillations. The left-most wave form in Fig. 3(a) shows the temporal evolution of these self-oscillations for V_f, with the corresponding power spectra shown in the center panel and the trajectory in the phase space $(V_f, \dot{V}_f)$ on the right. As V_d is further increased, a very clear period-doubling sequence to chaos is observed as shown in Figs. 3(b)–3(d). The self-oscillation of V_f bifurcates first into the state of $2P$ [Fig. 3(b)], then into that of $4P$ [Fig. 3(c)], and then rapidly into a chaotic state [Fig. 3(d)], where $2P$ and $4P$ signify the states of periods 2 and 4, respectively. That further bifurcations fail to be observed in experiments is due to the restraint of noise in the system. Similar results have also been obtained but on the upper branch of the I-V curve on another device.[8]

After entering into the chaotic region, the discharge displays alternatively chaotic and certain periodic-window behavior, depending on the control parameters. Figures 4(a)–4(c) show several periodic windows observed in experiments. When V_d is increased to a certain threshold value, the chaotic discharge state changes suddenly into the periodic window of $7P$ [Fig. 4(a)]. As V_d is further increased, the periodic window of $7P$ is replaced by the chaotic state gradually rather than suddenly. This situation appears again for the ensuing periodic windows of $5P$ [Fig. 4(b)] and $3P$ [Fig. 4(c)] when we continue to increase V_d. Moreover, it is found that the periodic window of $3P$ occupies the largest interval of V_d.

In the periodic window of $3P$, a fine structure is also observed, as shown in Fig. 5. It is evident that this is the period-6 state which has bifurcated from the period-3 state through period doubling. Here, in fact, is a secondary period-doubling sequence which makes the transition from the periodic window of $3P$ to the chaotic state and can be designated as the 3×2^nP $(n=0,1,2,\ldots)$ sequence.[9] Again, the noise of the system prevents us from observing further bifurcations.

The above results contain all three steps of routes to chaos through period doubling: main bifurcation sequence $(2^nP, n=0,1,2,\ldots)$; periodic windows embedded in the chaotic region; and secondary bifurcation sequences occurring in the periodic windows.

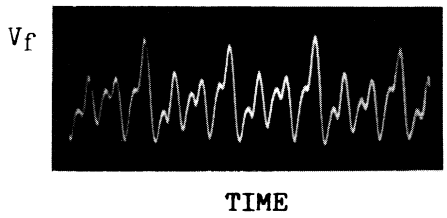

FIG. 5. Bifurcations occurring in the periodic window of $3P$. $I_f=240$ A, $P_a=1.7\times10^{-3}$ Torr, and $V_d=10.10$ V.

Another route to chaos commonly observed is intermittent chaos. In experiments, intermittent chaos possesses a considerable variety of evolution wave forms, depending on the control parameters of the discharge. Figures 6(a)–6(c) show only a set of experimental results for intermittent chaos. The temporal evolution of the discharge state [Fig. 6(a)] displays clearly intermittent chaotic behavior, with an inner and outer trajectory in phase space as shown in Fig. 6(c). Random jumps occur from one trajectory to the other frequently. The evolution of intermittent chaos is very sensitive to changes of the control parameters.

Here, the plasma system displaying chaotic behavior is not driven by any external periodic forces, it is only a dc discharge. The plasma oscillation observed is a kind of self-generated oscillation. Because there is no defined frequency that can be referred to, the fundamental frequency of self-oscillations is determined only by the peaks on the power spectra. Figures 7(a)–7(c) show the relationship of the frequency with the control parameters of the discharge. The frequency changes continuously as the control parameters change: The frequency increases with an increase of V_d, I_f, or P_a; when period doubling occurs, the increase in frequency becomes smooth. In Fig. 7(a), the arrows pointing upwards and downwards indicate the onset and offset of plasma self-oscillations, respectively. Hysteresis is also present here, but it occurs in the frequency. The oscillations in the regions

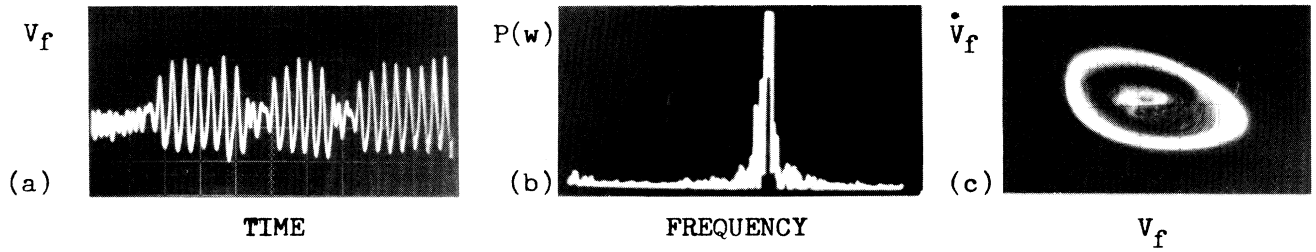

FIG. 6. Intermittent chaos observed at $I_f=240$ A, $P_a=9.8\times10^{-4}$ Torr, and $V_d=11.90$ V. (a) Temporal evolution of V_f; (b) power spectrum; (c) trajectory in phase space $(V_f, \dot{V}_f)$.

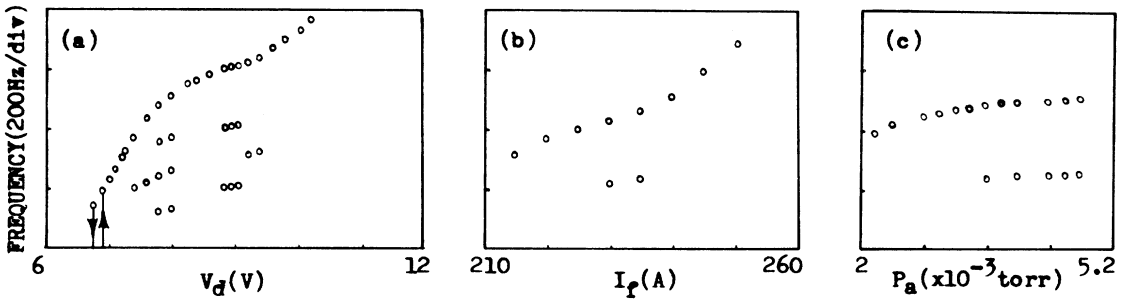

FIG. 7. The dependences of the fundamental frequency of plasma self-oscillations on (a) V_d at $I_f=240$ A and $P_a=2.4\times10^{-3}$ Torr; (b) I_f at $V_d=8.10$ V and $P_a=5.4\times10^{-3}$ Torr; and (c) P_a at $V_d=8.90$ V and $I_f=220$ A.

of A and B are essentially chaotic. In addition, the bifurcation diagram in Fig. 7(a) is surprisingly similar to results of 1D maps.[10]

Bifurcation and chaos can be described by systems of ordinary differential equations. In order to describe the undriven chaos, one needs autonomous differential equations which involve at least three independent variables. In the experiments, there are at least three variables, the discharge current, plasma potential, and electron density, which all display chaotic behavior. These three variables may probably compose a set of autonomous equations with the general form

$$dx_i/dt=f_i(x_1,x_2,x_3;\mu_1,\mu_2,\mu_3),\quad i=1,2,3, \tag{1}$$

where the x_i $(i=1,2,3)$ represent the above three variables, and μ_1, μ_2, and μ_3 represent the control parameters of V_d, I_f, and P_a, respectively. The right-hand side of Eq. (1) is the nonlinear functions. Equations of such form have been well investigated and shown to display chaotic behavior.[3,11] In addition, the correlation dimension of plasma undriven chaos computed from the time series of V_f[12] is about 2.6. This result (to be published elsewhere) supports the idea that the experimental results should be described by autonomous equations of at least three variables.

In conclusion, we have reported experimental observations of deterministic chaos occurring in an undriven plasma. A period-doubling sequence and intermittency have been found as the two routes to chaos. Fine structures such as periodic windows and bifurcations in the windows have also been observed. The experimental results were surprisingly similar to the dynamics of 1D maps, and should be described by a set of autonomous differential equations involving at least three variables.

The authors would like to thank S. B. Zheng and Y. P. Chen for helpful discussions and S. T. Yang and Y. Q. Luo for enthusiastic aid with equipment, and to acknowledge invaluable assistance by our colleagues in the CT-6B tokamak team. This work was supported in part by the Chinese National Science Foundation.

[1]E. N. Lorenz, J. Atmos. Sci. **20**, 130 (1963).

[2]*Evolution of Order and Chaos in Physics, Chemistry, and Biology,* edited by H. Haken, Springer Series in Synergetics Vol. 17 (Springer-Verlag, Berlin, 1982).

[3]*Directions in Chaos,* edited by Hao Bai-Lin (World Scientific, Singapore, 1988), Vols. 1 and 2.

[4]P. S. Linsay, Phys. Rev. Lett. **47**, 1349 (1981); J. Testa, J. Pérez, and C. Jeffries, Phys. Rev. Lett. **48**, 714 (1982).

[5]J. R. Tredicce *et al.*, Phys. Rev. A **34**, 2073 (1986); Hongjun Zhang *et al.*, in Ref. 3, Vol. 2, p. 46.

[6]P. Y. Cheung and A. Y. Wong, Phys. Rev. Lett. **59**, 551 (1987).

[7]P. Y. Cheung, S. Donovan, and A. Y. Wong, Phys. Rev. Lett. **61**, 1360 (1988).

[8]Y. Jiang, H. Wang, and C. Yu, Chin. Phys. Lett. **5**, 489 (1988).

[9]Hao Bai-Lin, Prog. Phys. **3**, 329 (1983) (in Chinese).

[10]P. Collet and J. P. Eckmann, *Iterated Maps on the Interval as Dynamical Systems* (Birkhäuser, Boston, 1980).

[11]Hao Bai-Lin, *Chaos* (World Scientific, Singapore, 1984).

[12]N. Gershenfeld, in Ref. 3, Vol. 2, p. 310.

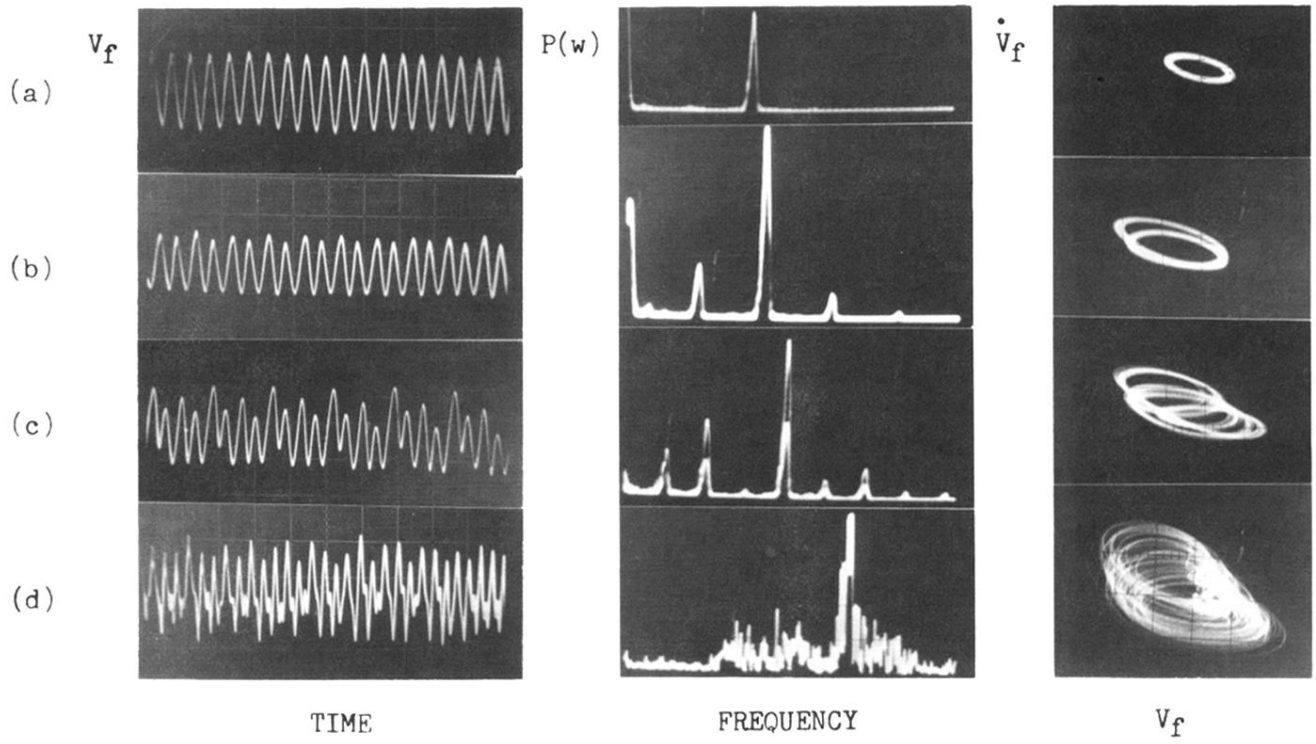

FIG. 3. A period-doubling sequence to chaos observed at $I_f = 240$ A, $P_a = 2.4 \times 10^{-3}$ Torr. The temporal evolution of the potential of unbiased probes, the power spectra, and the trajectory in phase space $(V_f, \dot{V}_f)$ is shown. (a) $V_d = 7.35$ V; (b) $V_d = 7.55$ V; (c) $V_d = 7.80$ V; (d) $V_d = 8.44$ V.

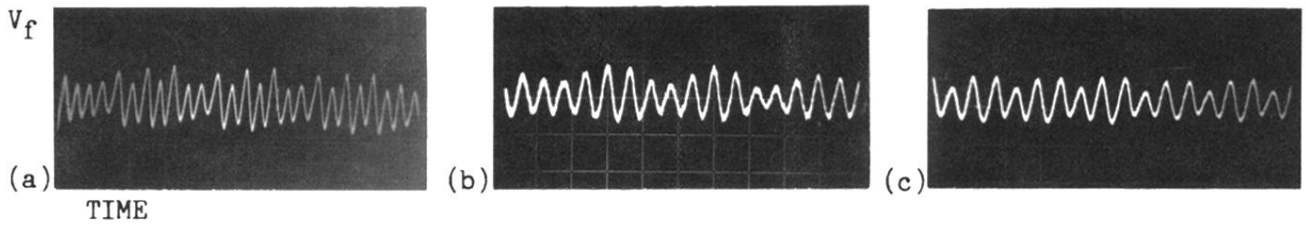

FIG. 4. Some periodic windows observed at $I_f = 240$ A, $P_a = (1\text{–}1.7) \times 10^{-3}$ Torr. (a) $7P$: $V_d = 9.39$ V; (b) $5P$: $V_d = 9.60$ V; (c) $3P$: $V_d = 9.96$ V.

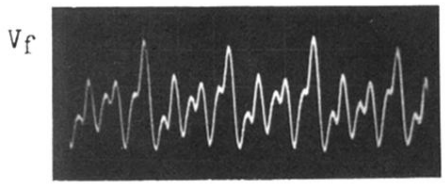

FIG. 5. Bifurcations occurring in the periodic window of $3P$. $I_f = 240$ A, $P_a = 1.7 \times 10^{-3}$ Torr, and $V_d = 10.10$ V.

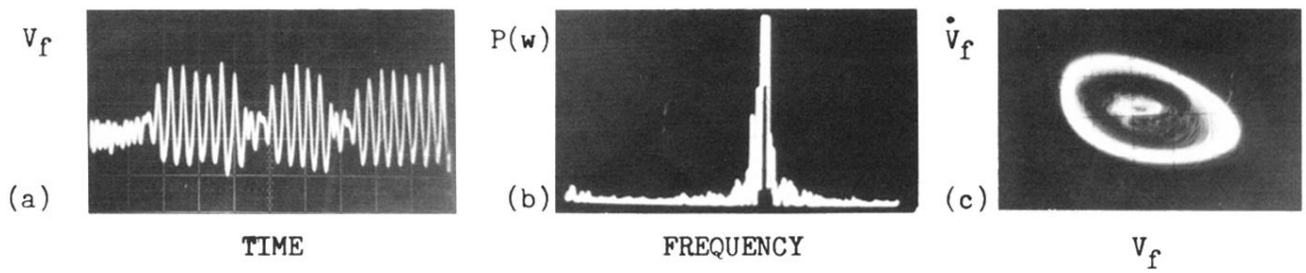

FIG. 6. Intermittent chaos observed at $I_f = 240$ A, $P_a = 9.8 \times 10^{-4}$ Torr, and $V_d = 11.90$ V. (a) Temporal evolution of V_f; (b) power spectrum; (c) trajectory in phase space $(V_f, \dot{V}_f)$.